Int. J. Heat Mass Transfer. Vol. 29, No. 5, pp. 753–759, 1986
Printed in Great Britain

0017–9310/86 $3.00 + 0.00
Pergamon Journals Ltd.

Effects of flow inertia on vertical, natural convection in saturated, porous media

K. S. CHEN and J. R. HO

Department of Mechnical Engineering, National Sun Yat-Sen University, Kaohsiung, Taiwan 800, R.O.C.

(*Received* 30 *July* 1985 *and in final form* 25 *November* 1985)

Abstract—An analytical study is made for the effect of flow inertia on vertical, natural convection in saturated, porous media. Within the framework of boundary-layer approximations, Forchheimer's model was transformed into a set of non-similar equations. Effects of flow inertia are measured and examined in terms of the dimensionless inertia parameter $\xi = Gr_x Fo_x$, where Gr_x is the local Grashof number of determined by the bulk properties of saturated porous media, and Fo_x is a new dimensionless parameter governed by the microstructure of porous matrix. The non-similar solutions are presented and discussed for two types of flow: (1) the uniform heat flux surface; and (2) plane plume flows. Results show that thermal boundary layer in the non-Darcy regime is thicker than the corresponding pure-Darcy flow. In addition, the local wall heat fluxes for the first case and the maximum temperature gradient for the second case decrease with increasing ξ.

1. INTRODUCTION

TRANSPORT processes in porous media occur in many different fields and engineering applications such as petroleum reservoirs and geothermal operations, packed-bed chemical reactors, transpiration cooling, food drying and building insulation. This has led to extensive researches into the subject. Most studies deal primarily with the mathematical formulation based on Darcy's law, which neglects the inertia effect on the flow and heat transfer through porous media [1, 2]. This also includes the boundary-layer treatment of Darcy's law, see refs. [3–12]. However, the effect of flow inertia is expected to become more significant when the pore Reynolds number is large. This is especially the case in high Rayleigh number regime or in high-porosity media.

In spite of the importance of inertia effect in common practice, no serious efforts have been devoted to its study until recently. Vafai and Tien [13] investigated the inertia and boundary effects in forced convection over a horizontal, heated plate based on the volume-average technique. Vafai [14] studied the inertia effect in a similar problem but also considered the variable-porosity effect. For natural convection in saturated, porous media, Plumb and Huenefeld [15] studied the inertia effect along an isothermal, vertical plate based on the Ergun model using the boundary-layer approximations and obtained the similarity solutions. Bejan and Poulikakos [16] studied the similar problems (including uniform heat flux plate) based on the Forchheimer's model. However, the scales chosen were based on the order of magnitude analysis in the limit where the inertia force was predominant. As a result, the Rayleigh number used in ref. [16] is different from the conventional one [10, 15] and the Nusselt number expression differs markedly from its counterpart in the pure-Darcy limit. Moreover, the effect of flow inertia was not examined when the similarity solutions did not exist.

It is the purpose of this study to examine the inertia effect on vertical, natural convection, boundary-layer flows in saturated, porous media, specifically, for a class of non-similar problems in terms of the inertia parameter ξ. In all cases, the inertia effect on the flow and heat transfer characteristics are presented and discussed for both the Darcy regime $\xi = 0$ and the non-Darcy regime $\xi \neq 0$. Comparisons of local heat flux in the limits of $\xi \to 0$ and $\xi \to \infty$ with other studies are also made.

2. MATHEMATICAL FORMULATION

Consider the problem of steady, natural convection in a porous medium adjacent to a vertical, impermeable plate (Fig. 1) with a prescribed surface temperature different from that at infinity. The origin of the coordinate system is placed on the impermeable plate where its temperature begins to deviate from that of the ambient temperature with x and y denoting the coordinates parallel and normal to the bounding

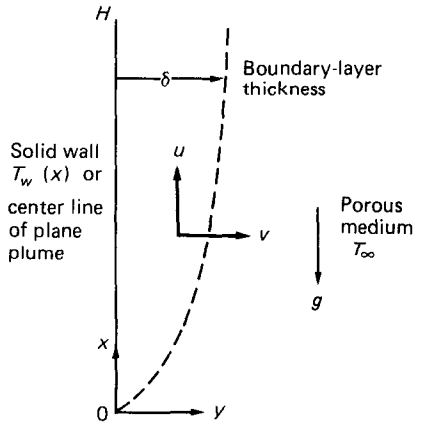

FIG. 1. Schematic of natural convection near a vertical plate.

NOMENCLATURE

A constant in equation (10)
C_p specific heat of saturated porous medium
f dimensionless streamfunction defined in equation (14a)
Fo_x dimensionless number defined in equation (21)
g gravitational acceleration; also dimensionless function defined in equation (22)
Gr_x local Grashof number defined in equation (20)
H characteristic height of porous medium
K permeability of porous medium
k thermal conductivity of saturated porous medium
Nu_x local Nusselt number defined in equation (36)
p pressure
Pr Prandtl number
q local wall heat flux
q_c convection energy in boundary layer, defined in equation (37)
Ra_x local Rayleigh number defined in equation (13)
T temperature
u vertical velocity component
v horizontal velocity component
x coordinate parallel to vertical plate
y coordinate normal to vertical plate.

Greek symbols
α thermal diffusivity
δ boundary-layer thickness
ξ inertia parameter; dimensionless coordinate
η dimensionless coordinate
β thermal expansion coefficient
ρ fluid density
μ fluid viscosity
λ constant in equation (10)
ϕ dimensionless function defined in equation (23)
ψ streamfunction
θ dimensionless temperature.

Subscripts
max maximum value
0 condition when $\lambda = 0$
∞ value in the ambient.

surface. If we assume that: (1) properties of the fluid and the porous medium are everywhere isotropic and homogeneous; (2) Forchheimer's model is used for the momentum equation and (3) the Boussinesq approximation is employed, then the governing equations in a Cartesian coordinate system are given by [2]

$$\frac{\partial u}{\partial x}+\frac{\partial v}{\partial y}=0 \tag{1}$$

$$\frac{\mu}{K}u+b\rho u\sqrt{u^2+v^2}=-\frac{\partial p'}{\partial x}+\rho g\beta(T-T_\infty) \tag{2}$$

$$\frac{\mu}{K}v+b\rho v\sqrt{u^2+v^2}=-\frac{\partial p'}{\partial y} \tag{3}$$

$$u\frac{\partial T}{\partial x}+v\frac{\partial T}{\partial y}=\alpha\left(\frac{\partial^2 T}{\partial x^2}+\frac{\partial^2 T}{\partial y^2}\right) \tag{4}$$

where p' is the pressure difference between the actual static pressure and the local hydrostatic one; ρ, μ and β are the density, viscosity and the thermal expansion coefficient of the fluid, respectively; K is the permeability of the porous matrix, $\alpha = k/(\rho C_p)$ is the equivalent thermal diffusivity. Note that the second term on the LHS of equation (2) or (3) is the inertia force in Forchheimer's model, which is omitted in Darcy's law, and b is a non-negative constant depending on the microstructure of the porous matrix (the units of b are m^{-1}), see ref. [2]. Following the order of magnitude analysis in the boundary layer [9], for example,

$$\frac{u}{H}=\frac{v}{\delta}$$

$$\frac{\partial}{\partial x}\ll\frac{\partial}{\partial y},\quad \frac{\partial^2}{\partial x^2}\ll\frac{\partial^2}{\partial y^2}$$

the boundary-layer equations for the porous layer along the heated, vertical plate are

$$\frac{\partial u}{\partial x}+\frac{\partial v}{\partial y}=0 \tag{5}$$

$$u\left(1+\frac{bK\rho}{\mu}u\right)=-\frac{K}{\mu}\left\{\frac{\partial p'}{\partial x}-\rho g\beta(T-T_\infty)\right\} \tag{6}$$

$$0=\frac{\partial p'}{\partial y}\quad\text{or}\quad p'=p'(x) \tag{7}$$

$$u\frac{\partial T}{\partial x}+v\frac{\partial T}{\partial y}=\alpha\frac{\partial^2 T}{\partial y^2}. \tag{8}$$

Note that we have made use of the fact that

$$u\sqrt{u^2+v^2}=u^2\sqrt{1+(u/v)^2}\simeq u^2$$

in equation (6). Eliminating p' from equations (6) and (7) yields

$$\frac{\partial T}{\partial y}=\frac{\mu}{\rho g\beta K}\frac{\partial u}{\partial y}+\frac{b}{g\beta}\frac{\partial u^2}{\partial y}. \tag{9}$$

The boundary conditions for equations (5), (8) and (9) are

$$y = 0: v = 0, \quad T = T_w = T_\infty + Ax^\lambda \tag{10}$$

$$y = \infty: u = 0, \quad T = T_\infty. \tag{11}$$

In equation (10), the wall temperature is a power function of x; A and λ are constants. By suitable choice of λ, the problem can be related to the natural convection adjacent to isothermal plate, uniform heat flux plate or plane plume generated from a line heating source, as will be described later.

The following variables are used to transform the (x, y) coordinates to dimensionless $(\xi(x), \eta(x, y))$ forms

$$\eta = \frac{y}{x} Ra_x^{1/2} \tag{12a}$$

$$\xi = \xi(x) \tag{12b}$$

where

$$Ra_x = \rho g \beta K (T_w - T_\infty) x / \mu\alpha. \tag{13}$$

The coordinate $\xi(x)$ is so chosen that x does not appear explicitly in either the transformed equation or the transformed boundary condition. In addition, the dimensionless streamfunction $f(\xi, \eta)$ and the dimensionless temperature function $\theta(\xi, \eta)$ are defined, respectively, as

$$f(\xi, \eta) = \frac{\psi(x, y)}{\alpha} Ra_x^{-1/2} \tag{14a}$$

$$\theta(\xi, \eta) = \frac{T - T_\infty}{T_w - T_\infty} \tag{14b}$$

where $\psi(x, y)$ is the streamfunction and

$$u = \frac{\partial \psi}{\partial y}, \quad v = -\frac{\partial \psi}{\partial x}. \tag{15}$$

Substitute equations (12)–(15) into equations (5), (8) and (9) to obtain

$$\theta' - f'' = \xi \frac{\mathrm{d} f'^2}{\mathrm{d}\eta} \tag{16}$$

$$\theta'' + \tfrac{1}{2}(1+\lambda) f\theta' - \lambda f'\theta = \lambda\xi \left(f' \frac{\partial \theta}{\partial \xi} - \theta' \frac{\partial f}{\partial \xi} \right). \tag{17}$$

The transformed boundary conditions are

$$\eta = 0: \theta(\xi, 0) = 1 \tag{18a}$$

$$\frac{1+\lambda}{2} f(\xi, 0) + \lambda\xi \frac{\partial f}{\partial \xi} = 0 \tag{18b}$$

$$\eta = \infty: \theta(\xi, \infty) = 0, \quad f'(\xi, \infty) = 0. \tag{19a, b}$$

In these equations, primes denote partial differentiation with respect to η, and ξ is

$$\xi(x) = Gr_x Fo_x = (Ra_x / Pr) Fo_x \tag{20}$$

where Pr is the Prandtl number, Gr_x is the Grashof number, and Fo_x is a new dimensionless number defined by

$$Fo_x = Kb/x. \tag{21}$$

It can be seen that the inertia parameter ξ is the product of Gr_x and Fo_x. The former measures the local vigour of the flow, while the latter depends on the microstructure of the porous matrix [2].

Equations (16)–(19) show that the problem does not, in general, permit a similarity solution, except that: (1) $\xi = 0$, namely, flow inertia is neglected as in the Darcy regime, see ref. [10]; or (2) ξ = non-zero constant, that is, ξ does not depend on x. From equations (10) and (20), the second condition can be satisfied only if $\lambda = 0$ and corresponds to the natural convection adjacent to an isothermal, vertical plate, see ref. [15].

For $\lambda \neq 0$, the problems are non-similar and the local non-similarity procedures described in refs. [19, 20] are employed to solve equations (16)–(19). Introduce two new functions

$$g(\xi, \eta) = \frac{\partial f}{\partial \xi} \tag{22}$$

$$\phi(\xi, \eta) = \frac{\partial \theta}{\partial \xi}. \tag{23}$$

Substituting equations (22)–(23) into equation (17) yields

$$\theta'' + \frac{1+\lambda}{2} f\theta' - \lambda f'\theta = \lambda\xi(f'\phi - \theta' g). \tag{24}$$

Integrate equation (16) with respect to η and using the boundary condition (19b) to yield

$$\theta - f' = \xi f'^2. \tag{25}$$

Differentiate equations (24) and (25) with respect to ξ and use relations (22) and (23) yielding

$$\phi - g' - f'^2 = 2\xi f' g' \tag{26}$$

$$\phi'' + \frac{1+3\lambda}{2} g\theta' + \frac{1+\lambda}{2} f\phi' - \lambda g'\theta - 2\lambda f'\phi - \lambda\xi(g'\phi - \phi' g) = \lambda\xi \left(f' \frac{\partial \phi}{\partial \xi} - \theta' \frac{\partial g}{\partial \xi} \right). \tag{27}$$

The boundary conditions for the above two equations can be obtained in a similar way and are in the forms of

$$\eta = 0: \phi(\xi, 0) = 0$$

$$g(\xi, 0) = -\frac{2\lambda}{1+\lambda} g(\xi, 0) - \frac{2\lambda\xi}{1+\lambda} \frac{\partial g}{\partial \xi} \tag{28}$$

$$\eta = \infty: \phi(\xi, \infty) = 0. \tag{29}$$

To the first level of approximation, all the terms involving the ξ-derivative in equations (26)–(29) are neglected. Therefore, we have two auxiliary equations

$$\phi - g' - f'^2 = 2\xi f' g' \tag{30}$$

$$\phi'' + \frac{1+3\lambda}{2} g\theta' + \frac{1+\lambda}{2} f\phi' - \lambda g'\theta - 2\lambda f'\phi = \lambda\xi(g'\phi - \phi' g) \tag{31}$$

with boundary conditions

$$\eta = 0: g(\xi, 0) = 0, \quad \phi(\xi, 0) = 0 \tag{32}$$

$$\eta = \infty: \phi(\xi, \infty) = 0. \tag{33}$$

The local heat flux along the surface is calculated from

$$q = -k\left(\frac{\partial T}{\partial y}\right)_{y=0}$$

$$= kA^{3/2}\left(\frac{\rho K g\beta}{\mu\alpha}\right)^{1/2} x^{(3\lambda-1)/2}[-\theta'(0)] \quad (34)$$

which can be rewritten as

$$Nu_x = [-\theta'(0)]\, Ra_x^{1/2} \quad (35)$$

where Nu is the local Nusselt number defined by

$$Nu_x = \frac{qx}{k\Delta T} = \frac{qx}{k(T_w - T_\infty)}. \quad (36)$$

The amount of energy convected in the boundary region is

$$q_c(x) = \rho C_p A\left(\frac{\rho g\beta K A\alpha}{\mu}\right)^{1/2} x^{(3\lambda+1)/2}\int_0^\infty f'\theta\, d\eta. \quad (37)$$

Equations (16)–(19) and equations (30)–(33) form four coupled differential equations. For a fixed ξ, they can be treated as a set of ordinary differential equations of the similarity type, and can be integrated numerically by the Runge–Kutta method in conjunction with the Newton–Raphson iterative scheme [18, 19].

In what follows results for two types of flow, depending on the surface conditions, will be presented. In the first, local heat flux along the vertical plate is constant. As can be seen from equation (34), the first case is obtained by setting $\lambda = 1/3$. In the second, a plane plume will be examined. This case is obtained by setting $\lambda = -1/3$. As seen from equation (37), the convected energy in the boundary layer of plane plume is independent of x-direction.

3. RESULTS AND DISCUSSIONS

The dimensionless temperature profile $\theta'(\xi, \eta)$ and the vertical velocity component $f'(\xi, \eta)$ are presented in Figs. 2(a) and (b) for the case of uniform heat flux condition ($\lambda = 1/3$). In the figures, the inertia parameter ξ varies between 0 and 100. Notice that $\lambda = 0$ corresponds to the pure Darcy flow. It can be seen from Fig. 2 that as ξ increases $\theta'(\xi, 0)$ and $f'(\xi, 0)$ decrease, and thermal boundary-layer thickness increases accordingly. That is, the neglect of flow inertia in the momentum equation will result in overpredicting the local wall heat flux. From equation (35) the dimensionless heat flux can be expressed by

$$Nu_x/Ra_x^{1/2} = [-\theta'(0)]. \quad (38)$$

The values of $[-\theta'(0)]$ depend on the ξ-parameter. These functional dependencies are listed in Table 1 and plotted in Fig. 3. It is shown in Fig. 3 that $[-\theta'(0)]$ decreases as ξ increases.

Cheng and Minkowycz [10] investigated the problem based on the Darcy's law, i.e. $\xi = 0$. In terms of the present notation, they obtained

$$Nu_x/Ra_x^{1/2} = 0.679 \quad (39)$$

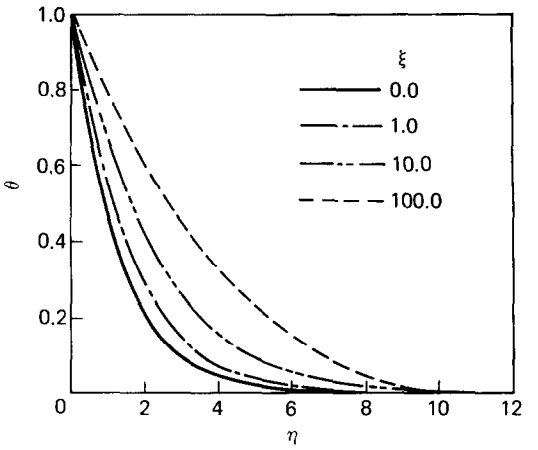

FIG. 2(a). Dimensionless temperature profile for uniform heat flux plate.

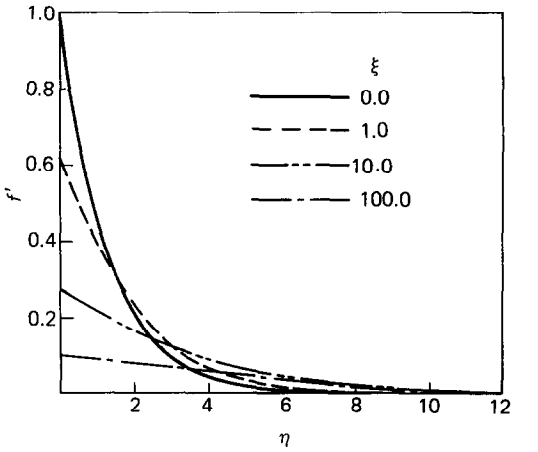

FIG. 2(b). Dimensionless vertical velocity profile for uniform heat flux plate.

for uniform heat flux surface condition. Equation (39) is shown as a dashed line in Fig. 3. It is evident that equation (39) is the limiting solution ($\xi \to 0$) of the present study.

Bejan and Poulikakos [16] investigated the same problem based on Forchheimer's model. As mentioned

Table 1. Values of calculated $[-\theta'(0)]$ and θ'_{max} for vertical natural convection in porous media

ξ	$Nu_x/Ra_x^{1/2} = [-\theta'(0)]$ uniform heat flux plate, $\lambda = 1/3$	$-\theta'_{max}$ plane plume $\lambda = -1/3$
0.0	0.6788	0.3143
0.001	0.6773	0.3141
0.01	0.6749	0.3126
0.1	0.6532	0.3002
1.0	0.5497	0.2453
5.0	0.4274	0.1863
10.0	0.3820	0.1616
50.0	0.2751	0.1185
100.0	0.2355	0.0958

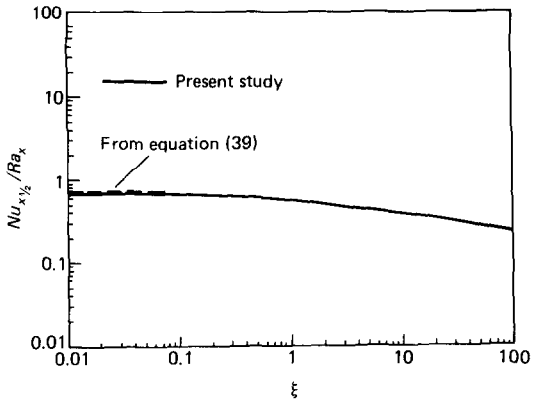

FIG. 3. $Nu_x/Ra_x^{1/2}$ vs ξ for uniform heat flux plate.

earlier, they used different boundary-layer scales, which were based on the limit when $\xi \to \infty$. In the present notation, they obtained

$$Nu_x/Ra_x^{2/3} = 0.695\,\xi^{-1/3}. \tag{40}$$

Equation (40) shows that Nu_x depends on $Ra_x^{2/3}$. This differs fundamentally from the present study and that of Cheng and Minkowycz [10] in which Nu_x depends on $Ra_x^{1/2}$.

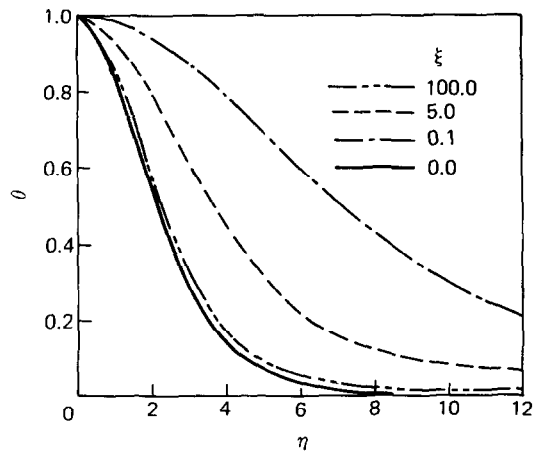

FIG. 4(a). Dimensionless temperature profile for plane plume.

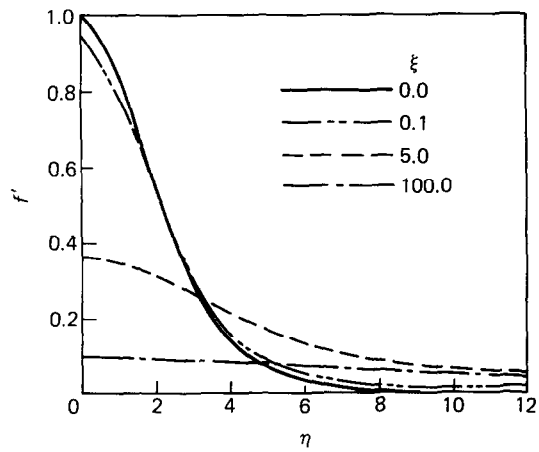

FIG. 4(b). Dimensionless vertical velocity profile for plane plume.

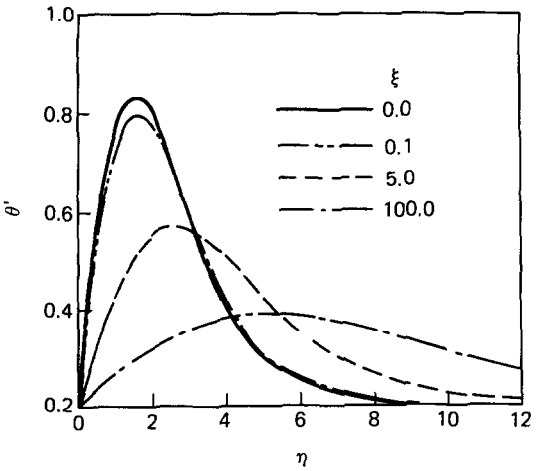

FIG. 5. Dependence of θ'_{max} on η and ξ for plane plume.

The plots of $\theta(\xi, \eta)$ and $f'(\xi, \eta)$ for the plane plume ($\lambda = -1/3$) are presented in Figs. 4(a) and (b), respectively. As in the case of uniform heat flux plate, $f'(\xi, 0)$ decreases and thermal boundary layer increases as ξ increases. Since $\theta'(\xi, 0) = 0$, an alternative way to examine the inertia effect on plane plume flow is by evaluating the local non-dimensional temperature gradient of

$$\theta'(\xi, \eta) = \frac{\partial \theta}{\partial \eta}.$$

The functional dependencies of θ' on ξ and η are listed in Table 1 and presented in Fig. 5. It can be seen from Fig. 5 that there is a maximum value of θ', called θ'_{max}, for each value of ξ; and that θ'_{max} decreases as ξ increases.

4. CONCLUSIONS

The effect of flow inertia on vertical, natural convection heat transfer in saturated, porous media has

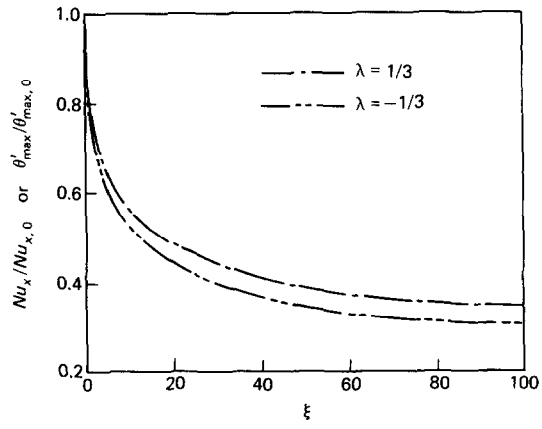

FIG. 6. The normalized Nu_x and θ'_{max} for: (1) $\lambda = 1/3$, uniform heat flux plate; and (2) $\lambda = -1/3$, plane plume.

been investigated by a local non-similarity method. Based on Forchheimer's model and boundary-layer approximations, the inertia effect is measured by the dimensionless parameter, ξ, which turns out to be the product of Gr_x and Fo_x. The former measures the local vigour of the flow and depends on the bulk properties of fluid and porous system, while the latter depends on the microstructure of the porous matrix.

Results are presented and discussed for two types of flow: the uniform heat flux plate and plane plume flows. In each case, the thermal boundary layer increases with increasing ξ. Effects of ξ on Nu_x and θ'_{max} are presented in Table 1 and Figs. 3 and 5. Figure 6 summarizes these relations by normalizing the Nu_x or θ'_{max} with respect to their corresponding pure-Darcy values. It can be seen that the normalized values decrease as ξ increases.

REFERENCES

1. J. Bear, *Dynamics of Fluids in Porous Medium.* American Elsevier, New York (1972).
2. P. Cheng, Heat transfer in geothermal reservoirs, *Adv. Heat Transfer* **14,** 1–105 (1979).
3. R. A. Wooding, Convection in a saturated porous medium at large Rayleigh number or Peclet number, *J. Fluid Mech.* **15,** 527–544 (1963).
4. J. W. Weber, The boundary layer regime for convection in a vertical porous layer, *Int. J. Heat Mass Transfer* **18,** 569–573 (1975).
5. P. G. Simpkins and P. A. Blythe, Convection in a porous layer, *Int. J. Heat Mass Transfer* **23,** 881–887 (1980).
6. P. A. Blythe and P. G. Simpkins, Convection in a porous layer for a temperature dependent viscosity, *Int. J. Heat Mass Transfer* **24,** 497–506 (1981).
7. P. A. Blythe, P. G. Daniels and P. G. Simpkins, Thermally driven cavity flows in porous media. I. The vertical boundary layer structure near the corners, *Proc. R. Soc.* **A380,** 119–136 (1982).
8. A. Bejan, Natural convection in a vertical cylindrical well filled with porous medium, *Int. J. Heat Mass Transfer* **23,** 726–729 (1980).
9. P. Cheng, Convective heat transfer in porous layer by integral methods, *Letters Heat Mass Transfer* **5,** 243–252 (1978).
10. P. Cheng and W. J. Minkowycz, Free convection about a vertical flat plate embedded in a porous medium with application to heat transfer from a dike, *J. geophys. Res.* **82,** 2040–2044 (1977).
11. W. J. Minkowycz and P. Cheng, Free convection about a vertical cylinder embedded in a porous medium, *Int. J. Heat Mass Transfer* **23,** 726–729 (1980).
12. Y. Joshi and B. Gebhart, Vertical natural convection flows in porous media: calculations of improved accuracy, *Int. J. Heat Mass Transfer* **27,** 69–75 (1984).
13. K. Vafai and C. L. Tien, Boundary and inertia effects on flow and heat transfer in porous media, *Int. J. Heat Mass Transfer* **24,** 195–203 (1980).
14. K. Vafai, Convective flow and heat transfer in variable-porosity media, *J. Fluid Mech.* **147,** 233–259 (1984).
15. O. A. Plumb and J. C. Huenefeld, Non-Darcy natural convection from heated surfaces in saturated porous media, *Int. J. Heat Mass Transfer* **24,** 765–768 (1981).
16. A. Bejan and D. Poulikakos, The non-Darcy regime for vertical boundary layer natural convection in a porous medium, *Int. J. Heat Mass Transfer* **27,** 717–722 (1984).
17. C. F. Dewey, Jr. and J. F. Gross, Exact similar solutions of the laminar boundary layer equations, *Adv. Heat Transfer* **4,** 317–346 (1967).
18. T. Cebeci and P. Bradshaw, *Momentum Transfer in Boundary Layer,* pp. 219–220. McGraw-Hill, New York (1977).
19. E. M. Sparrow, H. Quack and C. J. Boerner, Local non-similarity boundary-layer solutions, *AIAA J.* **8,** 1936–1942 (1970).
20. E. M. Sparrow and H. S. Yu, Local non-similarity thermal boundary-layer solutions, *J. Heat Transfer* **93,** 328–334 (1971).

EFFETS DE L'INERTIE SUR LA CONVECTION NATURELLE VERTICALE DANS LES MILIEUX POREUX SATURES

Résumé—On étudie analytiquement l'effet de l'inertie de l'écoulement sur la convection naturelle verticale dans les milieux poreux. Dans le cadre des approximations de la couche limite, le modèle de Forchheimer est transformé en un système d'équations non linéaires. Les effets de l'inertie sont évalués et examinés en fonction du paramètre adimensionnel d'inertie $\xi = Gr_x Fo_x$, où Gr_x est le nombre de Grashof local déterminé à partir des propriétes globales du milieu poreux et Fo_x est un nouveau paramètre adimensionnel gouverné par la microstructure de la matrice poreuse. Les solutions non similaires sont présentées et discutées pour deux types d'écoulement: (1) flux de chaleur uniforme sur la surface; et (2) écoulements de panache plans. Les résultats montrent que la couche limite thermique est dans le régime non-darcien, plus mince que l'écoulement correspondant selon Darcy. De plus, les flux locaux à la paroi pour le premier cas et le gradient maximal de température, pour le second cas, décroissent quand ξ augmente.

DER TRÄGHEITSEINFLUSS BEI VERTIKALER, NATÜRLICHER KONVEKTION IN DURCHTRÄNKTEN PORÖSEN MEDIEN

Zusammenfassung—Der Trägheitseinfluß bei vertikaler, natürlicher Konvektion in durchtränkten, porösen Medien wurde analytisch untersucht. Im Rahmen der Grenzschicht-Approximationen wurde Forchheimers Modell in einen Satz von unabhängigen Gleichungen formuliert. Der Trägheitseinfluß bei der Strömung wurde gemessen und mit Hilfe des dreidimensionalen Trägheitsparameters $\xi = Gr_x Fo_x$ überprüft. Dabei wird die lokale Grashof-Zahl Gr_x durch die mittleren Stoffeigenschaften der getränkten, porösen Medien bestimmt und ein neuer dimensionsloser Parameter Fo_x durch die Mikrostruktur des porösen Gefüges festgelegt. Die unabhängigen Lösungen werden dargelegt und für zwei Strömungsarten erörtert: (1) Strömung bei gleichförmiger Wärmestromdichte, (2) Strömung einer ebenen Auftriebsfahne. Die Ergebnisse zeigen, daß die thermische Grenzschicht außerhalb des Darcy-Bereiches dicker ist als bei der entsprechenden reinen Darcy-Strömung. Zusätzlich sinkt beim ersten Fall die örtliche Wandwärmestromdichte und im zweiten Fall der maximale Temperaturgradient bei anwachsendem ξ.

ВЛИЯНИЕ ИНЕРЦИОННЫХ СВОЙСТВ ПОТОКА НА ВЕРТИКАЛЬНУЮ ЕСТЕСТВЕННУЮ КОНВЕКЦИЮ В НАСЫЩЕННЫХ ПОРИСТЫХ СРЕДАХ

Аннотация—Аналитически исследовано влияние инерционных свойств потока на вертикальную естественную конвекцию в насыщенных пористых средах. В приближении погранслоя модель Форхаймера преобразуется к системе неавтомодельных уравнений. Влияние инерции учитывалось и анализировалось с помощью безразмерного параметра $\xi = Gr_x Fo_x$, где Gr_x—локальное число Грасгофа, определяемое объемными характеристиками насыщенных пористых сред, а Fo_x—новый безразмерный параметр, связанный с микроструктурой пористой матрицы. Найдены и проанализированы неавтомодельные решения для двух типов течений: (1) к поверхности подводится однородный тепловой поток и (2) плоские струи. Результаты показывают, что толщина теплового пограничного слоя для случая, не описываемого законом Дарси, больше, чем для случая, подчиняющегося закону Дарси. Кроме того, локальные тепловые потоки у стенки в первом случае и максимальный температурный градиент во втором уменьшаются с ростом ξ.